Content

Abstract

For orthopaedic, dental or craniofacial applications osteointegration is critical for short-term initial stability and long-term success of the implant.

Important efforts have been made in the past to optimize the osteointegration of titanium implants in bone-contact applications, focusing mainly on biofunctionalization methods of its surface to reduce healing times and accelerate integration into the host tissue.

In the present in vitro study a heparin binding peptide (FHRRIKA) and a recombinant fragment of fibronectin, which contains an heparin binding domain as well (HBII), have been covalently immobilized onto titanium.

Both the peptide and the recombinant protein fragment promoted the adhesion and proliferation of osteoblast-like cells (Saos-2) and fibroblasts (HFFs). In contrast, they only supported modest levels of cell spreading.

Titanium functionalized with the peptide stimulates the expression of both osteoblast- and fibroblast-related genes, while titanium functionalized with the protein fragment stimulates only osteoblastic differentiation genes, being this strategy more selective.

This study demonstrates that heparin-binding domains play an important role in a variety of biological processes, however it must be noted that surfaces coated with FHRRIKA or HBII did not reach the efficiency required for a material to be implanted. Nevertheless, the possibility of include in a single coating several cell surface receptors found in osteoblasts might be an interesting approach for developing novel biomaterial surfaces used in bone contact applications, in this coatings FHRRIKA or HBII could be included.

Acknowledgements

I would like to express my gratitude to Carles Mas and Jordi Guillem, my research supervisors, for their dedication, time, guidance, and useful critiques of this project. I would also like to thank BIBITE members, particularly Joanna, for their advice and assistance in keeping my progress on schedule and also for bringing a good mood to the lab every week. Special thanks are also extended to the Amase program and UPC for offering me the chance to be here and also for the resources in running the project.

My grateful thanks are also extended to my family and friends for their help and support.

Chapter 1

Literature review

1. Biomaterials

Each year, millions of devices are implanted into the human body to restore normal body function that has been diminished due to age, disease or trauma. [1]

In orthopaedics and dentistry, some diseases and injuries may cause hard damage to bone tissues, which might not be naturally fixed. The only solution in these cases is to remove the damaged part of bone and replace it by an artificial implant.

When designing an implant the biomaterials chosen must meet the mechanical, physical and chemical properties for the specific application, maintaining these properties throughout the time of performance of the implant without inducing an undesirable response. [1]

Metallic materials have a wide application in biomedical science, because they display unique features for the substitution of articulations and teeth. Ceramic and polymeric materials are not recommended in regions that are subjected to heavy loads, repeated heavy loads, or parts where pressure is concentrated; they do not have the mechanical properties required. Also metallic implants exhibit good corrosion resistance in physiological environment, good resistance to fatigue and wear and biocompatibility.

The main drawback of metallic biomaterials is their lack of bioactivity, which causes a slow osteointegration between the biomaterial and the surrounding tissue. This represents a serious problem, because osteointegration is critical for short-term initial stability and long-term success of the implant.

Osteointegration refers to a direct structural and functional connection between living bone and the surface of a load-carrying implant without interposition of non-bone tissue. [2] The host system can stimulate an immune reaction in response to the biomaterial and isolate the implant with a connective tissue; in that case the

implant is not well osteointegrated, leading to an unstable mechanical fixation and compromising the long-term success of the implant (Figure 1). The process of osteointegration reflects an anchorage mechanism whereby non-vital components can be reliably incorporated into living bone and which persist under all normal conditions of loading. [3]

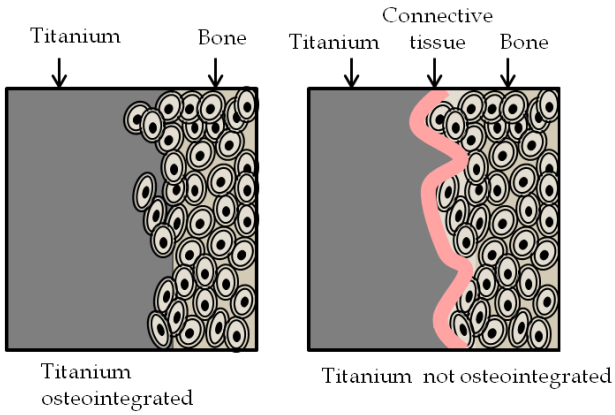

Figure 1 Titanium osteointegrated (left) and titanium not osteointegrated (right)

The acceptance, durability, and integration of an implant are ultimately dependent on the surface characteristics of the material and the events at the material-tissue interface. For this reason, in the last decade, surface modifications have been developed on metallic biomaterials to enhance its bioactivity with the aim of getting a faster osteointegration. [1]

2. Titanium

Since the 1960s, titanium has become a popular metallic biomaterial for many biomechanical applications because of its excellent properties. [4]

2.1. Properties

Commercially pure titanium (c.p. Ti) is a biologically inert biomaterial. It remains unchanged when implanted into human bodies, and does not promote any adverse reactions. However, the human body is able to recognize it as foreign and tries to isolate titanium by encasing it in fibrous tissues. [5]

Titanium surface is composed of a strong and stable oxide layer (TiO_2) that provides the ability to repair itself spontaneously by reoxidation when damaged, making that biomaterial biocompatible. It prevents the diffusion of the oxygen from the environment providing corrosion resistance to the material. And also avoids the release of particles to the organism. [4] [5]

Titanium is very light with a density of 4,5g/cm^3. Its mechanical properties are suitable to replace bone function. Its advantages include also lack of toxicity. Although the elastic modulus is higher compared to bone, causing sometimes

problems of stress shielding, its value is acceptable compared to other materials. [5]

2.2. Biomedical applications

Nowadays c.p. Ti is the dominant material for dental implants. [4] Titanium alloys, such as Ti6Al4V, are widely used as femoral stems and for other orthopaedic applications.

For hard tissue replacement, such as artificial bones and joint replacements, the low Young´s modulus of titanium and its alloys is viewed as a biomechanical advantage because it can result in smaller stress shielding compared to other implant materials. [4]

Titanium and its alloys are also used in cardiovascular implants, for example in prosthetic heart valves, protective cases for pacemakers, artificial hearts and circulatory devices. [6]

3. Surface modification of biomaterials

Surface modification is a process that changes a material's surface composition, structure or morphology leaving the bulk mechanical properties intact. [7]

Modifications of titanium surfaces can be grouped into 2 main groups: surface morphology and chemical surface modifications.

Modifications of surface morphology:

Structured titanium surfaces with different macro-, micro- and nano-topographies have been developed during the second half of the 20th century. Modifications of surface morphology are usually accomplished through etching (sulphuric acid or hydrochloric acid), grit-blasting (with Al_2O_3 or TiO_2), or a combination of both. [8]

Different degrees of surface roughness have shown to modify cellular behaviour. Also an increase in surface energy has been associated with increased surface roughness. The increase in surface energy improves the wettability of the implant surface, facilitating the adsorption of serum proteins and other biomolecules; it makes the surface more disposed to support the cascade of cellular events involved in the attachment, migration and differentiation of bone forming cells. [8]

Chemical surface modifications:

There are three groups of chemical surface modifications or coatings: modifications that use inorganic chemistry, modifications using organic molecules, and the combination of both. The strategy used in this project is organic surface modification.

Organic surface modifications and coatings

Placing a selected pattern of signals on the surface of the biomaterial, the process of tissue integration could be considerably accelerated. There are a number of molecules that appear particularly attractive from the perspective of cell adhesion and growth. [1]

Most of these molecules are proteins from the extracellular matrix (ECM) that are involved in cell communication, tissue repair and bone repair. Collagen, fibronectin, bone morphogenic proteins and growth factors from the bone matrix can be used as organic coatings, mimicking the native nano- and microenvironment for bone forming cells. [9]

These biologically active molecules can be attached to the surface of titanium implants through physical adsorption, covalent binding, nanomechanical incorporation and self-organizing organic layers. [1]

In this project molecules from the ECM are covalently bound to titanium.

3.1. Biofunctionalization

Biofunctionalization aims to modify the surface of a material with biological cues to control and improve the interaction between implant and tissue. Moreover, other specific objectives can be reached, for instance: triggering cell-selective response, resistance to bacterial attachment, reduction of the risk of inflammation or improvement of reliability and long-term performance of the device. [6]

In order to engineer a controlled biomaterial-host response to a biomolecular-modified surface, it is important to consider which receptors on the surface of the cell can connect with the biomolecules ligands. A popular method is incorporating molecules derived from ECM proteins or whole ECM proteins that interact with cell surface receptors. [1]

The ECM is a complex network of macromolecules composed of polysaccharides and a variety of proteins that are secreted by the cells and assembled into an organized network surrounding the cells within tissues. Domains on these proteins are recognized by cells stimulating attachment, migration, and/or differentiation. [1]

Cells interact with these domains on ECM proteins through transmembrane receptors; either the integrin family of cell surface receptors or cell surface proteoglycans (Figure 2).

Consequently biomolecules, such as peptides or proteins serve as ideal candidates to incorporate into the structure of synthetic materials.

In this project, cellular behaviour mediated by the interaction between heparin binding domains of biomolecules from ECM and cell surface proteoglycans is analyzed.

3.2. Interaction via proteoglycans

In contrast to integrin binding, cell surface proteoglycans bind to heparin binding domains mainly via electrostatic interactions. (Figure 2)

However, electrostatic forces are not sufficient and a steric fit is required between the proteoglycans and its binding site on the protein. [10]

This binding is highly dependent on the spatial location of the charges within the ligand. For example, the negatively charged carboxyl and sulfate groups present in proteoglycans interact with the positively charged heparin binding domains present in ECM proteins. This interaction is done through the amino acid sequence containing -X-B-B-X-B-X- where X and B represent hydrophobic and positively charged basic segment, respectively, of the heparin binding domain. [11] [12]

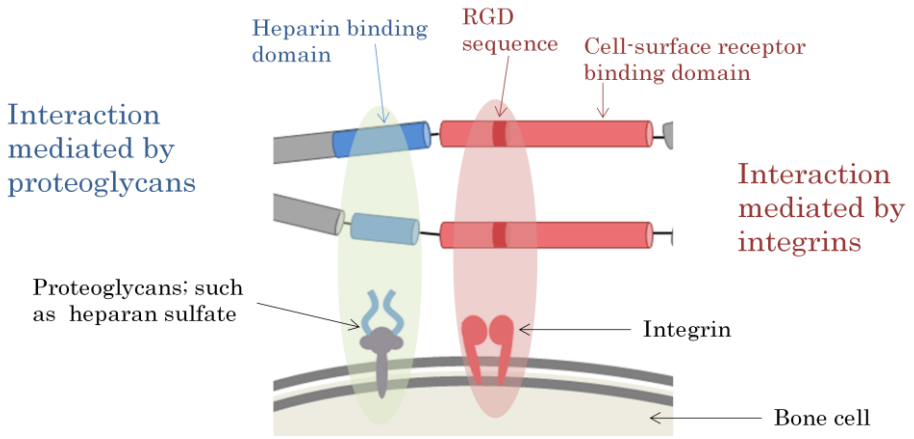

Figure 2 Integrin dependent and integrin-independent mechanisms implicated in cell attachment

3.3. Immobilization of biomolecules

In osseous tissue, the ECM is composed of about 90% collagenous and about 10% noncollagenous proteins. Some of the noncollagenous proteins include osteopontin, bone sialoprotein, fibronectin, vitronectin, osteonectin and thrombospondin.

Using a whole protein has some drawbacks, for instance: they potentially suffer from immunogenicity, have low solubility or are costly to extract and purify in large quantities. [7] [9]

One alternative is the use of ECM-derived peptides, and another one the use of recombinant fragments, which incorporate the minimal functional sequence of their parent protein. [9]

Compared to proteins, peptides are easily synthesized and purified in laboratories, are relatively inexpensive, are less susceptible to enzymatic degradation and less

likely to elicit an immunogenic response, in addition they do not denature under physiological conditions. [11][13]

However, the biological activity of short peptides is significantly lower than that of the complete protein, because of the absence of synergistic or complementary domains.

On the other hand, recombinant fragments of proteins offer an intermediate solution, reducing the main drawbacks associated to the use of full-length proteins and synthetic peptides.

In this project, the biomolecules from the ECM used are derived from the osseous tissue; one peptide and one recombinant fragment of protein.

3.4. Linear peptides

Peptides are designed to mimic a small linear bioactive domain found in proteins of the ECM; in that case the surface density and orientation of peptides can be controlled more simply than with native proteins.

3.4.1. FHRRIKA

FHRRIKA (Phe-His-Arg-Arg-Ile-Lys-Ala) is a peptide sequence from bone sialoprotein. This protein mainly interacts with mature bone cells, and is the major noncollagenous ECM protein secreted by osteoblasts. It is located in mineralized connective tissues and is up-regulated during bone formation. [1]

Up to the date some studies with this peptide have been carried out. Rezania and Healy (1999) [14] demonstrated enhanced osteoblast adhesion and mineralization on surfaces functionalized with mixtures of RGD and FHRRIKA compared with substrates with either RGD or FHRRIKA peptides alone.

Another study reveals that homogeneous FHRRIKA surfaces support cell adhesion and spreading, but they do not promote focal contact formation or cytoskeletal organization. However this peptide sequence improves clustering of the cytoskeleton when mixing with RGD. [1] [11]

3.5. Recombinant fragments of fibronectin

Recombinant fragments of protein offer an intermediate solution between using whole proteins or small sequences. They include all the regions of interest of the native protein for a specific biological function.

3.5.1. Heparin binding II recombinant fragment of fibronectin

Fibronectin is an abundant adhesive glycoprotein that is broadly distributed among vertebrates. It is a protein composed of modular subunits (Figure 3); these modules contain multiple binding sites. [15] Heparin binding II is the region of fibronectin used in this project.

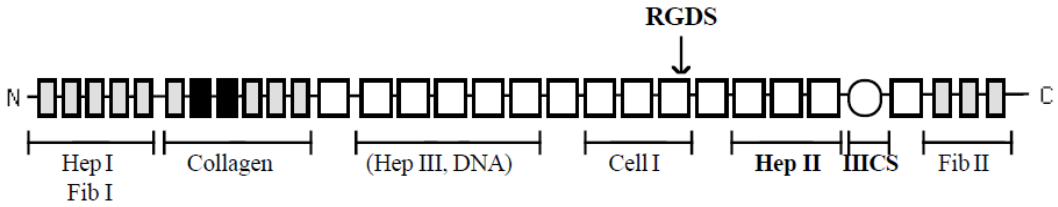

Figure 3 Schematic representation of fibronectin [16]

Previous studies showed that human bone cells have an attachment mechanism for the heparin-binding region; the attachment to this region is probably mediated by cell surface proteoglycans. However, they demonstrated that both integrin dependent and integrin-independent mechanisms have been implicated in cell attachment to the heparin binding domain II region of fibronectin. [16]

Other studies have demonstrated that some peptides sequences found in the heparin –binding domain have shown to be selective for osteoblast adhesion. [17]

Objectives

This project studies different methods for biofunctionalizing titanium surfaces, which are capable of causing specific cellular responses by biomolecular recognition. Here, a sequence of heparin binding peptide and a heparin binding recombinant fragment of fibronectin will be covalently immobilized onto smooth commercially pure titanium surfaces. The biofunctionalized surfaces are expected to elicit cell-specific biological responses.

The studied surfaces will be characterized by different techniques, such as contact angle measurements, SEM, XPS, AFM and white light interferometry. The biological response of the surfaces will be studied by means of cell adhesion and proliferation assays with osteoblasts and fibroblasts. In addition, the effects of the different biofunctionalized surfaces on the activation of HFFs and Saos-2 will be analyzed by measuring gene expression levels using real time PCR.

Objectives

Chapter 2

Materials and methods

4. Titanium samples

4.1. Samples preparation

Titanium grade 2 discs with a diameter of 10mm and thickness around 2mm were used for this study (Figure 4).

Bakelite powder was used for mounting the titanium samples by the LaboPress-3 (Struers, Denmark). Bakelite powder was put under pressure, and after curing, a hard plastic material containing the samples was formed.

The parameters set in the machine were:

Force: 15N
Heating time: 6 minutes
Heating temperature: 180ºC
Cooling time: 3 minutes

The titanium samples were then polished (Figure 4) on a Buehler Phoenix 4000 instrument system (Buehler, USA) down to mirror surface using various grit silicon carbide papers (Buehler, USA) and Al_2O_3 suspensions (Buehler, USA). (Table 1)

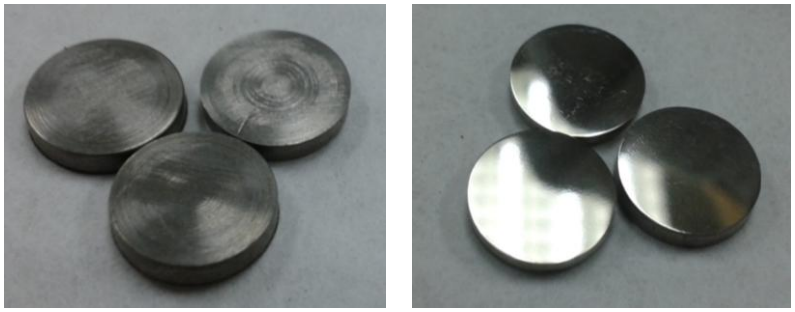

Figure 4 Titanium samples; trimmed (left) and polished (right)

Afterwards a manual handsaw was used to extract titanium samples from bakelites.

Samples were ultrasonically cleaned in cyclohexane, 2-propanol, distilled water, ethanol and acetone (Sigma-Aldrich, USA); finally they were dried with compressed air.

Table 1 Polishing steps for titanium samples

Paper/cloth	Time (minutes)	Lubricant	Head/Wheel rotational direction	Single sample force (lbs)	Speed (rpm)
SiC abrasive paper P800	10	Water	Contra	6	150
SiC abrasive paper P1200	20	Water	Contra	6	150
Velvet	60	Alumina 1 micron suspension	Contra	11	100
Velvet	60	Alumina 0,05 micron suspension	Contra	11	100
Velvet	30	Water	Contra	11	100

5. Surface activation treatment

Passivation treatments provide a controlled and uniformly oxidized surface state. The passivation leads to a dense and stable oxide film and improve corrosion resistance (decreases ion release).

The passivation procedure involves nitric acid, eliminating contaminants from the surface. It has however, practically no influence on the surface topography of titanium surfaces. The resulting layer of this chemical treatment is a TiO_2 film with a thickness of two to six nanometres. [18]

Oxidation of titanium surfaces was performed by immersing the samples into a 65% acid nitric solution (v/v) (Sigma-Aldrich, USA) for 1h at room temperature. Thereafter, they were abundantly rinsed successively in milliQ water, ethanol and acetone. Finally they were dried with compressed air.

6. Silanization of the samples

For the immobilization onto passivated surfaces the metallic samples were first immersed in anhydrous toluene with (3-aminopropyl)triethoxysilane (APTES) (2%, v/v) (Sigma-Aldrich, USA) for 1h at 70ºC under nitrogen atmosphere.

Subsequently, titanium samples were ultrasonically agitated in toluene for 5min to remove non-covalently bound silanes. Then, they were cleaned by immersing them in toluene, 2-propanol, distilled water, ethanol and acetone (Sigma-Aldrich, USA), finally dried with compressed air.

Further, a crosslinker was bound to the samples by immersing them in 2mg/mL of 3-maleimidopropionic acid N-hydroxysuccinimide ester (Alfa Aesar, USA) in N,N-dimethylformamide (DMF) for 1h at room temperature.

Finally samples were washed with DMF, distilled water, ethanol and acetone, and dried with compressed air.

This method provides the covalent binding of biomolecules, which ensures stable anchoring of the molecules on the surface (Figure 5).

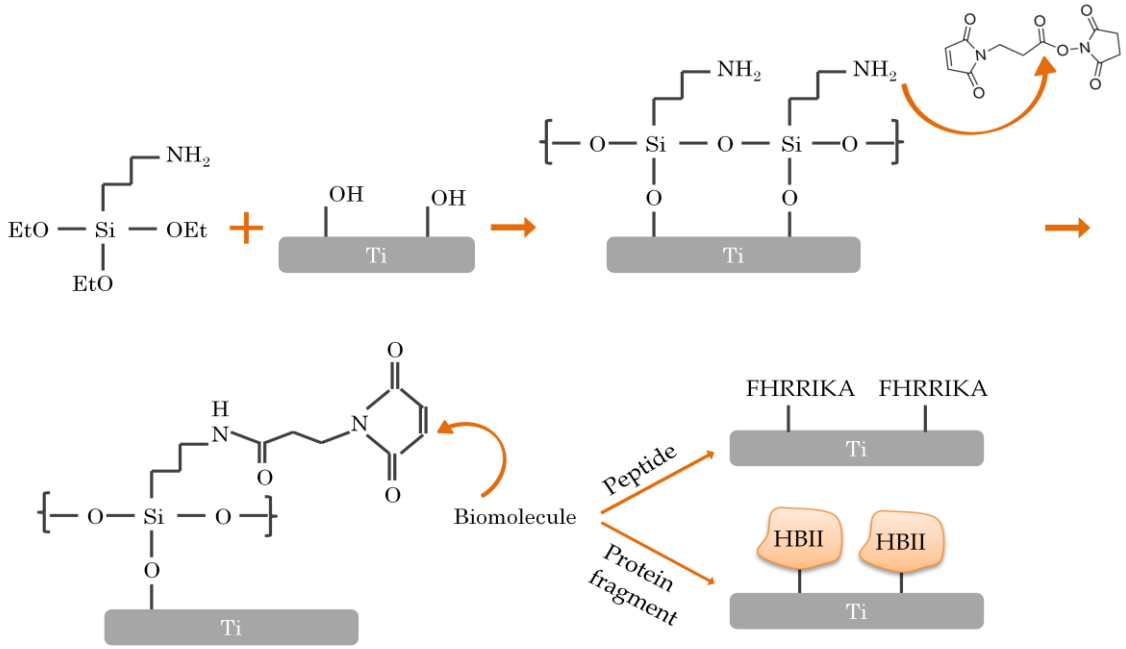

Figure 5 Silanization of the samples and immobilization of the biomolecules

7. Biomolecules immobilization

Both the FHRRIKA peptide and the HB II recombinant fragment of fibronectin were dissolved independently in phosphate buffered saline (PBS) at pH 6.5 at a concentration of 100µM and 100µg/ml, respectively. For the functionalization of the surfaces, a volume of 100µl/sample was deposited onto titanium samples overnight

at room temperature. After this time, samples were washed twice with PBS and dried with compressed air.

7.1. Linear peptide FHRRIKA

The sequence used for the heparin binding peptide is MPA-$(Ahx)_3$-FHRRIKA-NH_2 with a molecular weight of 1352,82g/mol.

Mercaptopropionic acid (MPA) is the anchoring part, a thiol group. The molecules also contains three units of 6-aminohexanoic acid (Ahx) as spacer, followed by the active sequence Phe-His-Arg-Arg-Ile-Lys-Ala (FHRRIKA).

This peptide was synthesized by means of solid-phase peptide synthesis [19] at the group of Biomaterials, Biomechanics and Tissue Engineering of the UPC.

7.2. Heparin binding recombinant fragments of fibronectin

The heparin binding recombinant fragment of protein used is the heparin binding II region of fibronectin; obtained following the process described in the PhD Thesis of Carolina Herranz Díez at the group of Biomaterials, Biomechanics and Tissue Engineering of the UPC [20], with the following sequence:

GPLGSPQFPGRQ AIPAPTDLKF TQVTPTSLSA QWTPPNVQLT GYRVRVTPKE KTGPMKEINL APDSSSVVVS GLMVATKYEV SVYALKDTLT SRPAQGVVTT LENVSPPRRA RVTDATETTI TISWRTKTET ITGFQVDAVP ANGQTPIQRT IKPDVRSYTI TGLQPGTDYK IYLYTLNDNA RSSPVVIDAS TAIDAPSNLR FLATTPNSLL VSWQPPRARI TGYIIKYEKP GSPPREVVPR PRPGVTEATI TGLEPGTEYT IYVIALKNNQ KSEPLIGRKK TAAAS

8. Methods for physico-chemical characterization

The biological response induced by biomaterials is related to its surface characteristics; such as, wettability, chemical composition, surface energy or surface topography, among others. For this reason is important to characterize the physico-chemical properties of the biofunctionalized materials developed.

8.1. Contact angle measurements

A characteristic that influences the response of a biomaterial when exposed to living tissues is the wettability, determined by measuring the contact angle at the liquid-solid interface (Figure 6).

The wettability refers to how the fluid adheres to the solid surface. And the surface tension of the solid is countered by a force at the solid-liquid interface, which pulls the liquid away from the surface of the dry solid. This force is known as the interfacial tension. [21]

The greater the attraction between the liquid and the solid, the lower the interfacial tension will be and the more spreading of the liquid over the surface of the solid.

Contact angle measurements on titanium surfaces were performed using a Contact Angle System OCA15 plus (Germany) and SCA20 software (Germany).

Contact angle was determined using the Sessile drop method with a drop volume of 3µl, using the Laplace–Young fitting approximation.

Ultrapure Milli-Q water (polar) and diiodomethane (non-polar) (Sigma-Aldrich, USA) liquids were used for the analysis of the wettability and the surface energy of the samples. All measurements were done at room temperature.

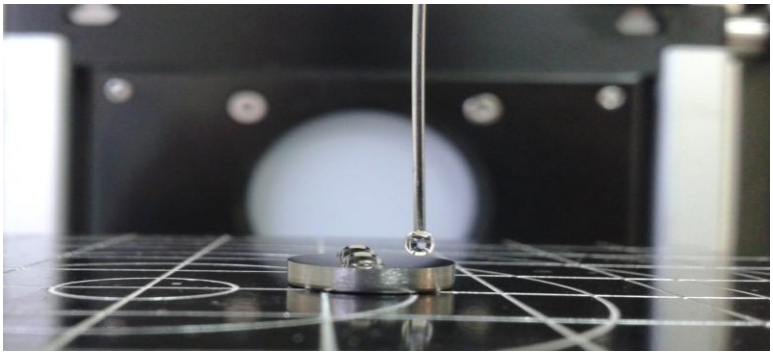

Figure 6 Contact angle technique

Theoretical description considers a thermodynamic equilibrium among the three phases; liquid (L), solid (S) and gas (G). The contact angle θ_C equilibrium is determined by the Young equation 1. Where energy between solid and gas is Y_{SG}, between solid and liquid is Y_{SL} and between liquid and gas is Y_{LG} (Figure 7).

$$Y_{SG} - Y_{SL} - Y_{LG}\cos\theta_C = 0 \quad (1)$$

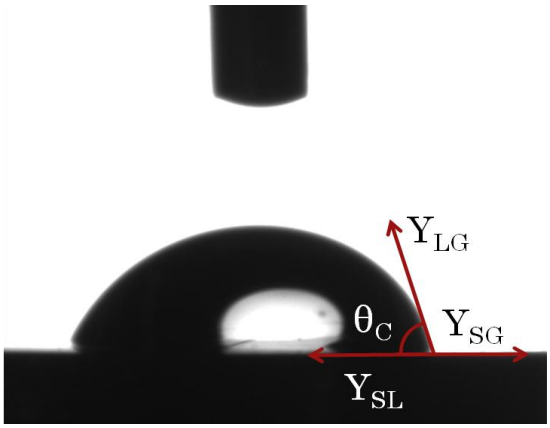

Figure 7 Contact angle of 73,0º on titanium passivated with acid nitric

Surface energy calculations were carried out using Fowkes equation 2 [22], using a polar and a non-polar liquids, to determine polar and non-polar components on the surfaces analyzed. Adhesion parameters of liquids used are tabulated by the same author (Strom et al in Table 2).

$$\gamma_L(1 + cos\theta) = 2\left[\sqrt{\gamma_L^d \gamma_S^d} + \sqrt{\gamma_L^p \gamma_S^p}\right] \quad (2)$$

Table 2 Characteristics of the liquids used [23]

Liquid	γ_L(mJ/m^2)	γ_L^d(mJ/m^2)	γ_L^p(mJ/m^2)
Ultrapure Milli-Q water	72,8	21,8	51,0
Diiodomethane	50,8	50,8	0,0

To get reliable results 3 drops per sample of each liquid were measured from 3 samples of each condition.

8.2. White light interferometry

Surface roughness evaluation is very important for characterizing the different functionalized surfaces, with this technique is possible to determine if the biomolecules immobilization affects the roughness of the material.

Vertical scanning interferometry (VSI) was used for surface profile measurement by analyzing a series of interference patterns of low coherence light with known optical path difference among them. This technique provides accuracy up to the nanometer level. [24]

The parameter analyzed is the arithmetic average height (R_a); defined as the average absolute deviation of the roughness irregularities from the mean line over one sampling length (equation 3). [25]

The measurements on titanium surfaces were performed using the Wyko® NT1100 Optical Profiling System and the software WykoVision® 32 (Veeco Instruments, USA).

$$R_a = \frac{1}{n}\sum_{i=1}^{n}|y_1| \quad (3)$$

8.3. SEM

A scanning electron microscope (SEM) is a type of microscope that produces images of a sample by scanning it with a focused beam of electrons. The electrons interact

with atoms in the sample, producing various signals that can be detected and that contain information about the sample's surface topography and composition. [26]

In this project SEM ZeissNeon 40 (Zeiss, Germany) was used to analyze qualitatively the effect of the polishing treatment onto the titanium surface.

8.4. AFM

Atomic force microscopy (AFM) was developed as a powerful tool to investigate the atomic-scale surface topographies of samples (Figure 8). It uses a sharp tip to probe the surface features by raster scanning. [27]

The Veeco Dimension 3100 Atomic Force Microscope (Veeco Instruments) was used with the software Nanoscope 7.30, also WSxM 5.0 was used for analyzing the data obtained.

The scans were done on tapping mode. Tapping mode provides higher resolution with minimum sample damage. It eliminates frictional forces by intermittently contacting the surface and oscillating with sufficient amplitude to prevent the tip from being trapped.

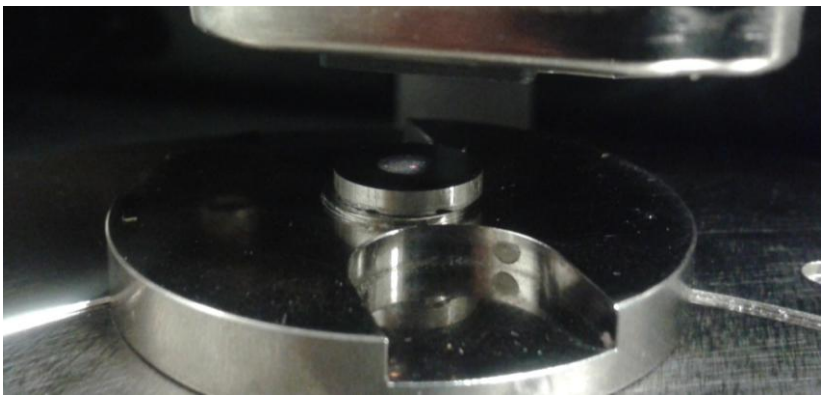

Figure 8 Sample in AFM

The parameter controls set were:

Scan size: 5,00µm
Scan rate: 0,501Hz
Samples/line: 512
Lines: 512
Aspect Ratio: 1,00
Integral Gain: 0,5
Proportional Gain: 0,5

And the limit used for the Z Range was 5,00µm.

Tapping mode uses a vibrating cantilever; as a result height data can be obtained from the changes in Z-axis displacement.

There is a phase difference between the measured signal and the drive signal, caused by interactions between probe and material. A 'phase image' can be formed using this data, which will indicate regions of different composition or phase in the material.

In this project AFM was used to analyze the distribution of the biomolecules on the titanium surfaces.

8.5. XPS

X-ray photoelectron spectroscopy (XPS) is a surface-sensitive quantitative spectroscopic technique that measures the elemental composition of the elements that exist within a material. XPS requires high vacuum conditions. [28]

XPS was used to analyse the surface chemistry of the different biofunctionalized samples and furthermore to analyse the stability of the biomolecules on the titanium surface. For this stability study, biofunctionalized samples were ultrasonically agitated in PBS for 1 hour. Then samples were rinsed in distilled water before the XPS analysis.

The elements evaluated were Ti, O, C, N, S and Si. These elements were chosen to identify the presence of the silane, the peptide and the recombinant fragment of the protein.

The chemical composition of the samples was analyzed using an XPS equipment (SPECS Surface Nano Analysis GmbH, Germany) and data was analyzed using CasaXPS software (Casa Software Ltd., UK).

9. Methods for biological characterization

9.1. Cell types

Two different cell types were used for analyzing the cellular responses of the biofunctionalized materials.

9.1.1. Saos-2

The human osteosarcoma cell line Saos-2 is widely used as a model system for human osteoblastic cells, since their first description in 1975.[29] Osteoblasts are important cells in the osteointegration of bone to the implant.

Some advantages for using this cell line are: its world wide availability, its good and well-documented characterization, the possibility to obtain large amounts of cells in short time and the fact that Saos-2 cells exhibit the entire differentiation features of osteoblastic cells.

Saos-2 cells were obtained from the American Type Culture Collection (ATCC, USA).

9.1.2. HFFs

Human foreskin fibroblasts (HFFs) primary cells (Millipore, USA) were also used.

Fibroblasts are the most common cells of connective tissue in humans and are important in wound repair mechanisms: fibrous encapsulation is caused by this type cells. Fibroblasts play a role in producing many of the ECM components essential for connective tissue.

9.2. Cell culture conditions

Saos-2 were cultured in McCoy's 5A medium (Sigma-Aldrich, USA) supplemented with 10% fetal bovine serum, penicillin-streptomycin (50U/ml and 50µg/ml, respectively), 2mM L-glutamine, 20mM HEPES and 1mM sodium pyruvate in a humidified atmosphere at 37ºC, 5% CO_2.

Fibroblasts were cultured in Dulbecco's modified eagle medium (DMEM) (Sigma-Aldrich, USA) supplemented with 10% fetal bovine serum, penicillin-streptomycin (50U/ml and 50µg/ml, respectively), 2mM L-glutamine and 20mM HEPES in a humidified atmosphere at 37ºC, 5% CO_2.

9.3. In vitro cellular assays

Different assays were done to evaluate cellular behaviour on the biofunctionalized samples, with both cell lines: osteoblast-like cells and fibroblasts.

9.3.1. Cell adhesion assay

Cells, either Saos-2 or HFFs, in serum-free McCoy's or DMEM, respectively, were seeded (11.400cells/cm^2) onto the titanium substrates of interest to the present study. Cells were allowed to adhere on these surfaces under standard cell culture conditions for 5h.

At the end of the incubation period; for the quantification of adherent cells 300µl M-PER™ Mammalian Protein Extraction Reagent was added, after rinsing and relocation of the samples to non-used wells.

The Cytotoxicity Detection Kit^{PLUS} (LDH) (Roche, Switzerland) was used to measure quantitatively the adhesion of human cells (HFFs and Saos-2).

Lactate dehydrogenase (LDH) is a stable cytoplasmic enzyme present in all cells. The amount of enzyme activity is correlated to the amount of cells. A calibration curve of increasing cell numbers was prepared to extrapolate the results.

To quantify cell numbers, 100µl from the lysis solution of each sample was mixed with the same amount of reaction mixture (catalyst in Dye solution (1:46)) in a 96-well plate and incubated less than 30min at room temperature, protecting the plate from light. Afterwards, 50µl of stop solution were added to each well, before measuring the absorbance at 492nm in a spectrophotometer (PowerWave XS Microplate, BioTek™, USA).

At the end of the incubation period; for the immunofluorescent staining assay adherent cells were fixed with 4% paraformaldehyde (PFA) in PBS for 20min, then washed twice in PBS and stored in PBS on the fridge until staining was done.

Staining of the adhered cells on adhesion assays was done to analyze the spreading and focal adhesion of cells onto the different substrates studied with both kinds of cells.

After fixation, samples were permeabilized with 0,05% Triton X-100 in wash buffer (20mM Glycine in PBS), to allow antibodies diffusion into the cell . After three washes with wash buffer, a blocking step with 1% BSA in wash buffer was done to avoid nonspecific interactions. Mouse anti-vinculin primary antibody (1:100) in 1% BSA was used to stain focal adhesions, followed by three washes. Then, Alexa Fluor 488 Goat anti-mouse IgG (1:2000) secondary antibody and Alexa Fluor 546 Phalloidin (1:300) in 0,05% Triton X-100 were added. Phalloidin stains actin filaments. After three more washes, DAPI in wash buffer was used to stain the nuclei. After three washes Mowiol was deposited onto the samples as mounting medium.

Nikon E600 microscope equipped with the camera DP72 (Olympus, Japan) and also the software Cell^F (Olympus, Japan) were used to acquire the images.

The excitation-wavelength region from 330nm to 380nm showed the cell nucleus in blue. From 510nm to 560nm actin filaments were seen in red. And focal adhesions were observed in green in the excitation-wavelength region from 450nm to 490nm.

ImageJ software was used to quantify spreading area of the cells.

9.3.2. Proliferation assay

Proliferation assays were done with the same conditions than adhesion assays, as explained in section 9.3.1. The unique difference was the samples sterilization in 70% ethanol for 30min after the blocking step. After that, samples were rinsed in sterile PBS three times. After 5h, medium was supplemented with FBS. The amount of cells was checked at four different points in time; 1day, 3days, 7days and 14days.

AlamarBlue (Invitrogen, USA) was used to measure quantitatively the proliferation of studied human cells (HFFs and Saos-2).

The active substrate of alamarBlue is non-toxic, cell permeable and blue in colour. When entering cells, is reduced to another compound which is red in colour and highly fluorescent. Viable cells continuously convert the active substrate, increasing the overall fluorescence and colour of the media surrounding cells.

With this method proliferation assays could be done evaluating cell viability always in the same samples, saving number of samples for the test and getting accurate results.

400µl of cell culture medium with 10% alamarBlue were added directly to cells. Then, samples were incubated for 1hour if working with more than 50.000cells and 3 hours if working with less than 50.000cells at 37ºC. Furthermore, two standard curves with known cell concentrations were seeded and analyzed (from 0cells up to 150.000cells) to determine the concentration of each sample. The standard curves should be done at two different incubation times because this test works with a wide range of cells. With lower cell concentration higher incubation time is required, and with higher cell concentration lower incubation time is needed, due to the fast reduction.

Then, fluorescence measurement was done with a Microplate Fluorescence Reader BioTek™ FLx800™ (BioTek Instruments, Inc, USA). The fluorescence excitation wavelength used was at 528nm and fluorescence emission at 590nm.

The proliferation was determined plotting fluorescence emission intensity versus cell concentration to correlate the samples concentrations from the standard curve. Larger fluorescence emission intensity values correlate to an increase in total metabolic activity from cells in the well.

9.3.3. Gene expression assay

Gene expression assay was done with the same conditions than adhesion assays, as explained in section 9.3.1. But using a higher cellular density, in this case a density of 36.400cells/cm^2 was seeded.

The gene expression was checked at three different time points; 5hours, 1day and 3days. The gens analyzed provide information related to the adhesion, ECM synthesis and remodelling of the cells seeded on the biofunctionalized surfaces (Table 3).

At each culture time, total RNA was extracted using RNeasy® Mini Kit (Qiagen, Germany). The amount of RNA was quantified using NanoDrop ND-1000 spectrophotometer (NanoDrop Technologies, USA). Then 130ng of RNA were retrotranscribed to cDNA using the QuantiTect Reverse Transcription Kit (Qiagen, Germany) following manufacturer's instructions. cDNA products were further diluted to 1ng/µl and used as RT-qPCR templates.

Applied Biosystems StepOnePlus Real-Time PCR machine (Applied Biosystems, USA) was used to analyze gene expression of the samples at each point in time. Negative controls and a standard curve were also performed to analyze the results obtained. Specificity of each RT-qPCR reaction was determined by melting curve analysis. All samples were normalized by the expression levels of ß-actin (reference gene) and fold changes were related to TCPS at 5h of culture as follows (equation 4):

$$FC = \frac{(E_{target})^{\Delta C_t target\ (TCPS5h-experimental)}}{(E_{reference})^{\Delta C_t reference\ (TCPS5h-experimental)}} \quad (4)$$

where Ct is the median value for the quantification cycle for the triplicate of each sample and E is the amplification efficiency, determined from the slope of the log-linear portion of the calibration curve, as: $E = 10^{[-1/slope]}$.

COL1A1, ACTB, ALP, OSC, BMP2 were selected for analyzing samples seeded with osteoblasts.

COL1A1, MMP2, ACTB, ACTA2 were selected for analyzing samples seeded with fibroblasts.

Table 3 DNA sequences of forward (fw) and reverse (rv) primers for the selected genes used [30]

Related function	Gene symbol	Gene title	Primer sequences (5′_3′)
ECM component	COL1A1	Collagen, type I, alpha 1	fw: AGGTCCCCCTGGAAAGAA rv: AATCCTCGAGCACCCTGA
ECM remodelling	MMP2	Matrix metallopeptidase 2 (Gelatinase A)	fw: CGGTTTTCTCGAATCCATGA rv: GGTATCCATCGCCATGCT
Endogenous control	ACTB	Actin, beta	fw: AGAGCTACGAGCTGCCTGAC rv: CGTGGATGCCACAGGACT
Matrix mineralization	ALP	Alkaline Phosphatase	fw: AGAACCCCAAAGGCCTTCTTC rv: CTTGGCTTTTCCTTCATGGT
Matrix mineralization	OSC	Bone Gamma-Carboxyglutamate (Gla) Protein (Osteocalcin)	fw: TGAGAGCCCTCACACTCCTC rv: ACCTTTGCTGGACTCTGCAC
Myofibroblastic marker	ACTA2	Actin, alpha 2, smooth muscle, aorta (α-SMA)	fw: CTGTTCCAGCCATCCTTCAT rv: TCATGATGCTGTTGTAGGTGGT
Bone formation marker	BMP2	Bone Morphogenetic Protein 2	fw: CAGACCACCGGTTGGAGA rv: CCCACTCGTTTCTGGTAGTTCT

10. Statistical analysis

All data presented in the study are given as mean values ± standard deviations. Statistical analysis was performed with Minitab (Minitab Inc, USA).

Significant differences between group means were analyzed by ANOVA test using Tukey's method to consider all possible pairwise differences of means at the same time. Mann-Whitney test was used as non-parametric test.

Confidence levels were set as 95% for all tests.

Chapter 3

Results and discussion

11. Results for physico-chemical characterization

11.1. Contact angle measurements

Water contact angle measurements show that passivation with nitric acid makes the titanium surface a bit more hydrophilic. In contrast, silanization with APTES increases water contact angle due to the hydrophobicity of the silane. Titanium surfaces with peptide and protein fragment show a similar hydrophilicity, with lower values of contact angle compared to silanized samples. The variations in wettability observed correlate well with the hydrophilicity of the coatings and confirm the process of functionalization.

For biofunctionalized surfaces and passivated titanium surfaces (negative control) contact angle is around 50º (Figure 9); hence the three surfaces used for the biological characterization have a similar hydrophilicity, thus the hydrophilicity is not going to have an effect on the biological behaviour of the different surfaces analyzed.

The contact angle values obtained with diiodomethane show very similar values for all the surfaces analyzed.

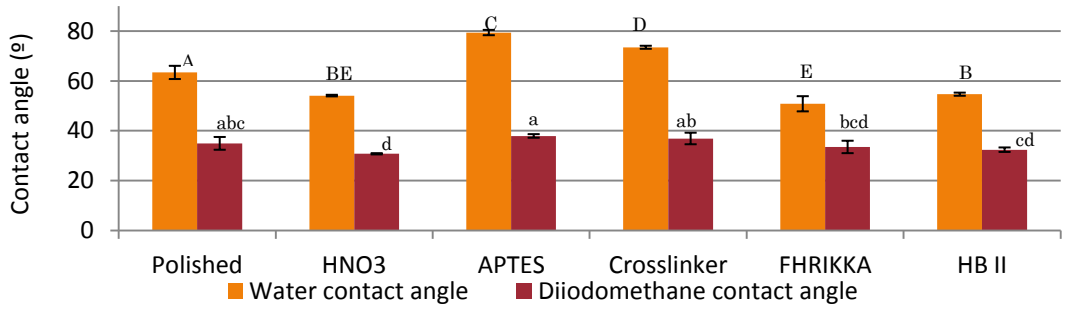

Figure 9 Contact angle measurements. Letters (A–E; a-d) denote statistically significant differences (P<0.05) between groups

In Figure 10 surface energy associated results are shown; the values for the three surfaces used for the biological characterization have similar surface energy, a bit higher the one with the peptide, due to a higher dispersive component. This data is highly correlated with water contact angle measurements because is obtained from Fowkes equation (equation 2).

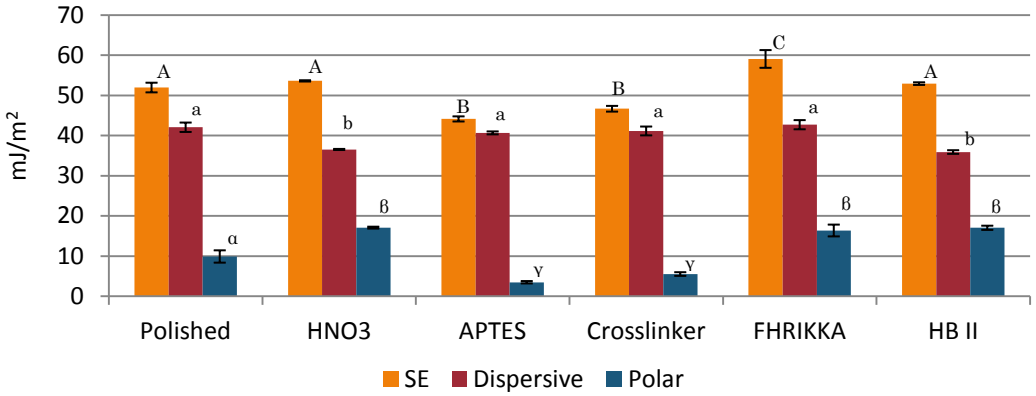

Figure 10 Surface energy, dispersive and polar components. Letters (A–C; a-b; α-γ) denote statistically significant differences (P<0.05) between groups

11.2. White light interferometry

Diminishing the roughness of the samples to a few nanometres by polishing yielded a more uniform surface.

The surface roughness can alter the process of osteointegration because cells react differently to smooth or rough surfaces. In general, fibroblasts and epithelial cells adhere more strongly to smooth surfaces, whereas osteoblasts have a better affinity to rough surfaces. Furthermore, surface roughness has an influence on cell migration and proliferation. [2]

When polishing trimmed titanium, the arithmetic average height of titanium is reduced to a few nanometres. The process of passivation does not show significant differences to the roughness of the surface. Neither do the biofunctionalization process (Table 4). Because of the similar roughness between samples, this parameter can be ruled out and biological behaviour will be due to the functionalized molecules.

Table 4 Arithmetic average height values (R_a). Letters (A–B) denote statistically significant differences (P<0.05) between groups

Samples	R_a (nm)	
Trimmed	1506,4 ± 797,8	A
Polished	28,1 ± 6,2	B
HNO_3	31,9 ± 9,5	B
FHRRIKA	25,9 ± 8,8	B
HB II	29,1 ± 4,1	B

11.3. SEM

In Figure 11 and Figure 12 the topography of titanium before and after polishing is shown. With that polishing process the whole surface of the samples is more uniform, and roughness effects are avoided. Moreover, passivation, silanization and biofunctionalization processes do not affect samples topography, which corroborates results obtained by VSI.

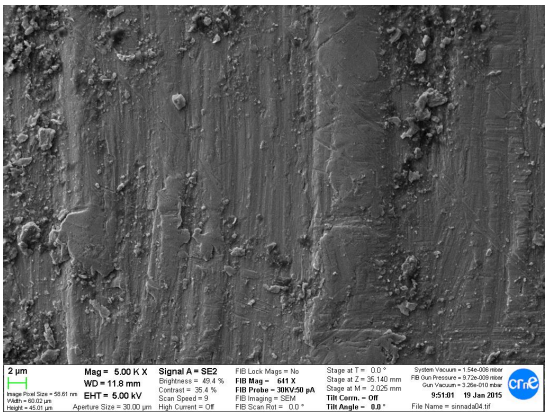

Figure 11 Topography of trimmed titanium sample

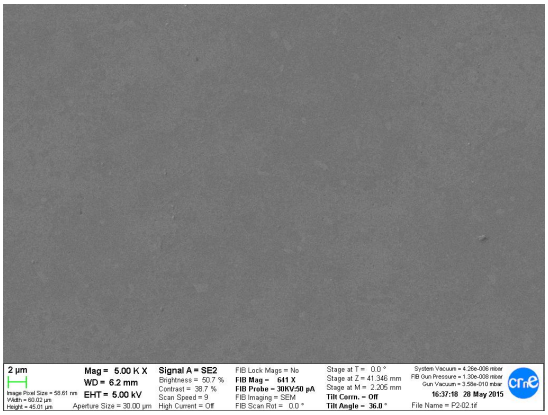

Figure 12 Topography of polished titanium sample

11.4. AFM

AFM images of the different surfaces are illustrated in Figure 13. Profiles of the height data reveal similar values for the different surfaces, as it was seen by interferometry. Profiles of the phase data show values of degrees very similar throughout the line for all the surfaces analyzed, indicating that all regions analyzed have only one homogenous layer on the material.

On the basis of XPS data, it is thus possible to confirm that the silanization process creates a full layer of silane over the titanium surface. However, on the biofunctionalized samples, it is not possible to univocally confirm the presence of a layer of biomolecules. To discriminate the layer of biomolecules from the previous

layer of silane, an AFM working on liquid mode would be preferable; however, this equipment was not available during the project.

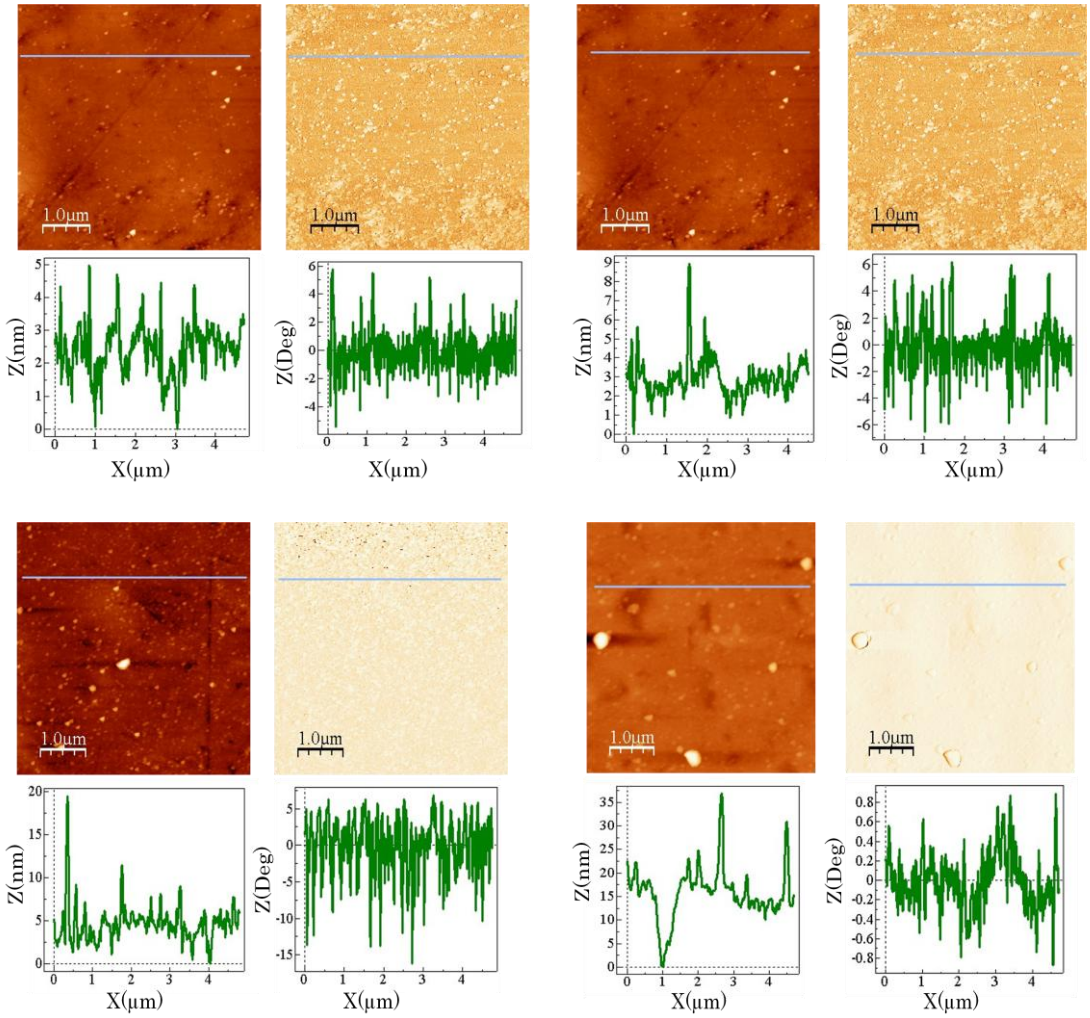

Figure 13 AFM height data and phase data images, and profiles of them. Up from left to right: Titanium passivated with HNO3, titanium silanized with APTES; down from left to right: titanium functionalized with FHRRIKA, titanium functionalized with HB II.

11.5. XPS

Atomic percentages of the analyzed surfaces are shown in Table 5. When the surfaces are silanized the amount of C, N and Si significantly increases, due to the deposition of a wide layer of silane on the titanium surface, while the detectable signal of Ti diminishes considerably.

When surfaces were functionalized with peptide or protein fragment, it could be observed that the amount of Si was reduced compared with silanized surfaces, whereas the amount of Ti increased. This observation can be explained by the loss of non-covalently bound silanes during the cleaning process.

Interestingly, analysis of the stability of the functionalization with the peptide (i.e. N 1s signals) reveals that the binding to the surface is very stable (FHRRIKA values vs. FHRRIKA 1H PBS), thus confirming that the peptide has been successfully bound on the titanium surface, and that this binding is stable.

In contrast, when analyzing the stability of the functionalization with the protein fragment, a decrease of the N amount can be detected (HB II values vs. HB II 1H PBS), which reveals that some extent of protein is detached from the surfaces during the stability treatments. Most likely, this is due to the fact that some protein fragments are bound covalently to titanium, but another fraction may be only physically adsorbed.

Table 5 Analysis of the chemical composition of Ti surfaces by XPS. Values are expressed as mean ± standard deviation.

Samples	**Composition (atomic %)**				
	C 1s	N 1s	O 1s	Si 2p	Ti 2p
HNO_3	28,4 ± 3,1	1,1 ± 0,1	52,8 ± 2,1	0,2 ± 0,1	17,6 ± 0,9
APTES	52,6 ± 1,6	7,9 ± 0,5	25,6 ± 1,6	11,8 ± 0,6	2,2 ± 1,1
FHRRIKA	42,3 ± 6,8	5,8 ± 0,2	39,1 ± 4,9	6,7 ± 0,5	6,2 ± 1,4
FHRRIKA 1H PBS	37,0 ± 0,9	5,3 ± 0,0	44,9 ± 0,6	6,6 ± 0,2	6,2 ± 0,1
HB II	50,3 ± 2,5	12,1 ± 0,3	30,5 ± 1,8	4,2 ± 0,4	2,9 ± 0,7
HB II 1H PBS	47,7 ± 3,4	9,1 ± 0,1	34,9 ± 2,3	4,9 ± 0,3	3,4 ± 1,0

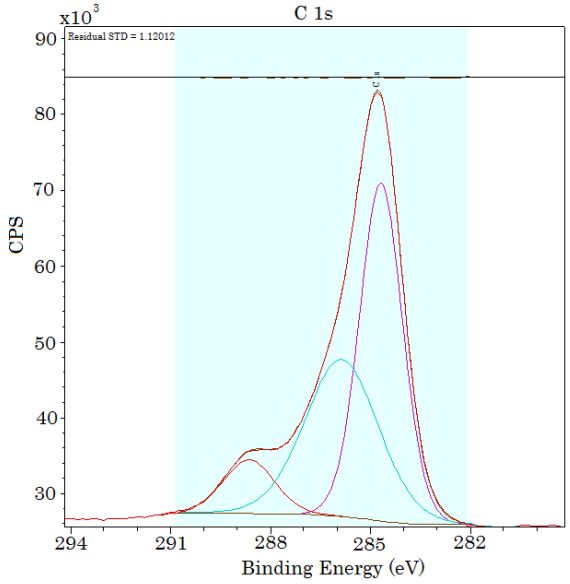

Figure 14 Deconvolution of C1s for titanium passivated with HNO_3

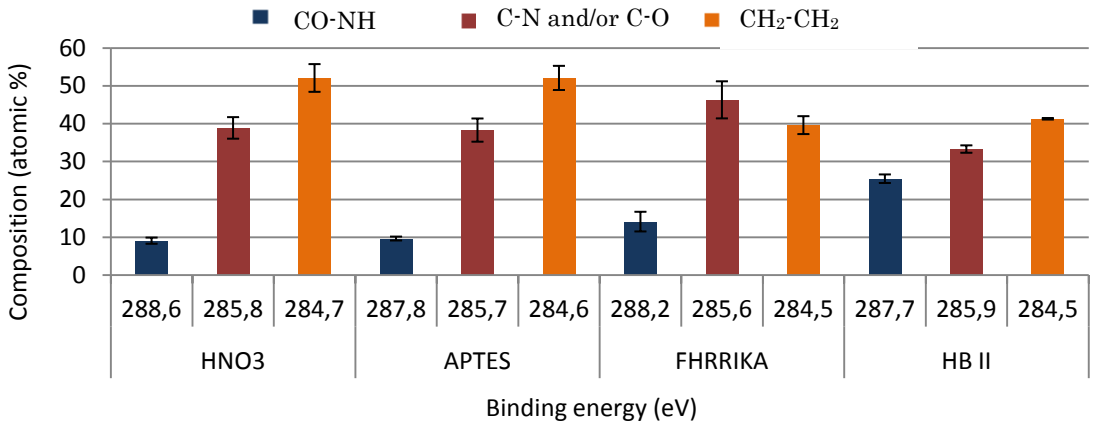

Figure 15 Chemical composition of the deconvolution of C1s

Figure 14 illustrates the 3 peaks obtained with the deconvolution of the C1s signal. Figure 15 shows the data obtained for the deconvolution of C1s for the different surfaces analyzed.

Deconvolution of the C 1s peak reveals 3 components: groups CO-NH around 288eV, bonds C-N and C-O around 285,5eV, and groups CH_2-CH_2 around 284,5eV.

It can be seen that the peak around 288eV increases for the biofunctionalized surfaces compared to controls. Since this peak corresponds to polar amide groups (CO-NH), its increase is consistent with the presence of the biomolecules. This increase is higher for the protein fragment than for the peptide; suggesting a higher amount of protein immobilized on the surfaces.

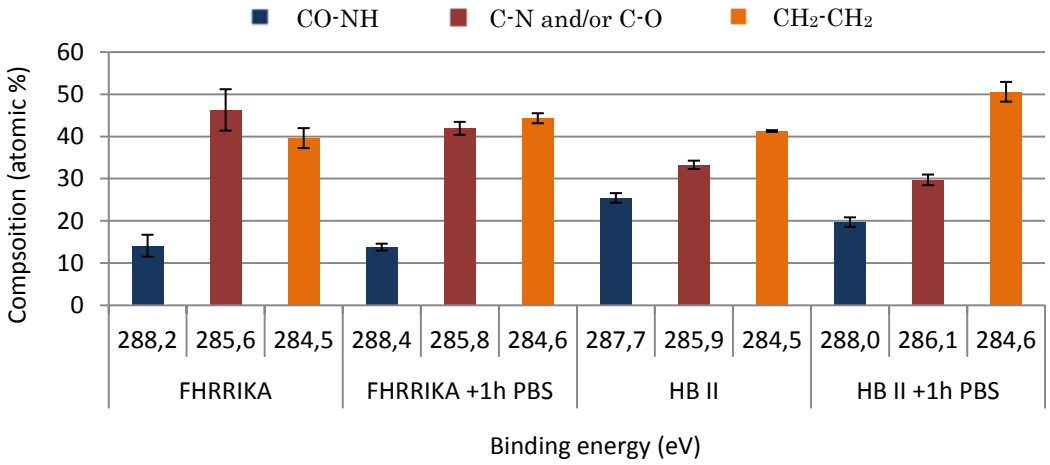

Figure 16 Chemical composition of the deconvolution of C1s for the stability study

In Figure 16 the stability of the biofunctionalized surfaces can be observed. Noteworthy, the peak around 288eV maintains its atomic % after the stability study for the samples coated with the peptide. On the contrary, on the samples

coated with the protein fragment this signal diminishes. This result corroborates the hypothesis that not all the protein fragment is covalently bound on the titanium samples.

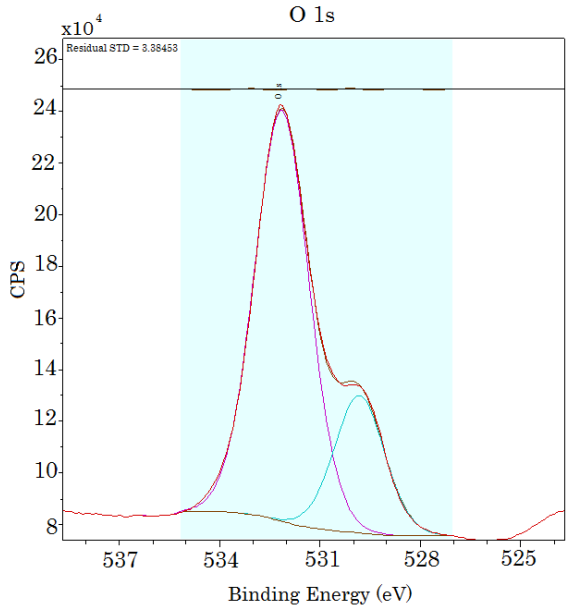

Figure 17 Deconvolution of O1s for titanium silanized

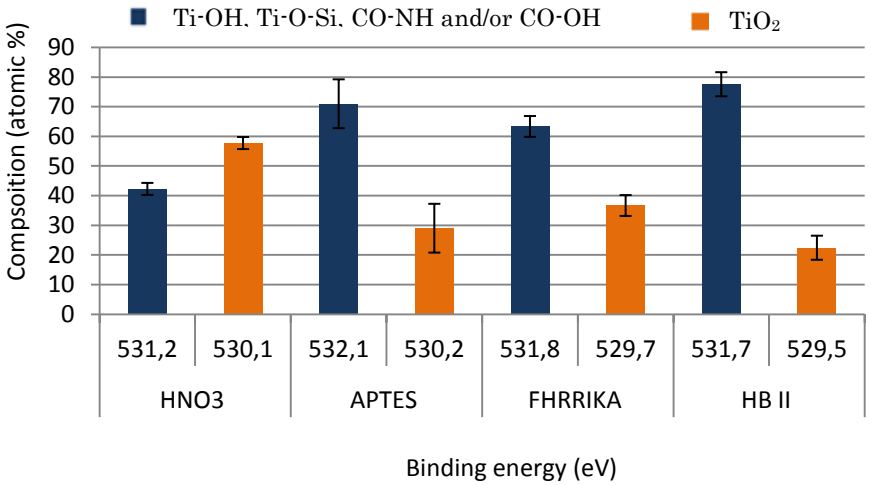

Figure 18 Chemical composition of the deconvolution of O1s for the analyzed surfaces

Figure 17 illustrates the 2 peaks obtained with the deconvolution of O1s. Figure 18 shows the data obtained for the deconvolution of O1s for the different surfaces.

Deconvolution of the O 1s peak reveals 2 components: groups Ti-OH around 532eV, and groups TiO_2 around 530eV.

HNO_3 samples have a TiO_2 peak at 530eV and a Ti-OH peak at 531eV.

The peak around 532eV increases after silanization with APTES. Such increase is correlated with the appearance of the Ti-O-Si bond. The subsequent binding of the

peptide or protein fragment is associated with the presence of amide groups (CO-NH), however this signal appears in the same region (532eV), and cannot be differentiated from the Ti-O-Si peak.

Thus, the stability of the biofunctionalized surfaces cannot be analyzed with the deconvolution of O1s, due to overlapping of the binding energies.

12. Results for biological characterization

12.1. Adhesion assay

Biofunctionalized surfaces increased the number of cells attached compared to control Ti surfaces for both cell types. After 5h of incubation surfaces biofunctionalized with the peptide support a similar level of adhesion for Saos-2 and HFFs. In contrast, the protein fragment clearly has a preferential binding-capacity for Saos-2 cells over HFFs (Figure 19).

Previous studies, Rezania and Healy (1999) [14] and Dalton et al. (1995) [16] demonstrated the binding capacity of osteoblasts in FHRRIKA and HB II biofunctionalized surfaces, respectively.

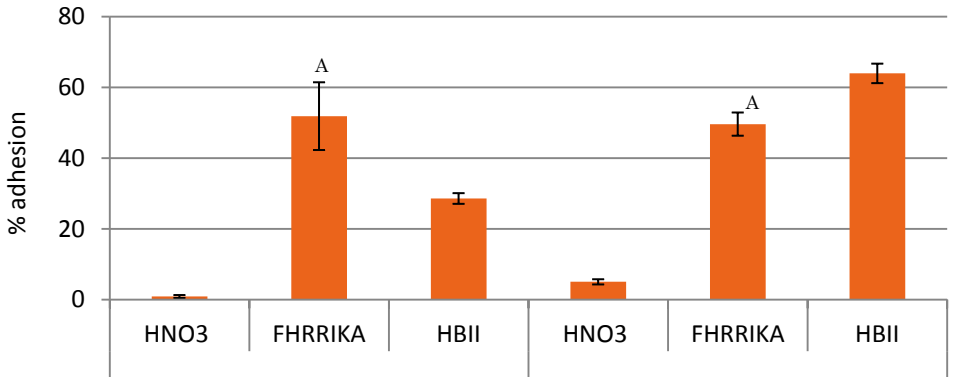

Figure 19 Adhesion test: cell attachment of Saos-2 and HFFs cells on Ti surfaces. Same letter indicates no statistically significant differences ($P < 0.05$) among the conditions.

The enhancement in cell adhesion due to the presence of the biomolecules was accompanied by an increase in the spreading of adherent cells. However, these values of cell area are not as high as they should be for a full spreading, indicating that heparin binding domains do not promote a complete phenotype of cell spreading (Figure 20). There were no statistically significant differences among the distinct biofunctionalized surfaces (Figure 20, Figure 21, Figure 22).

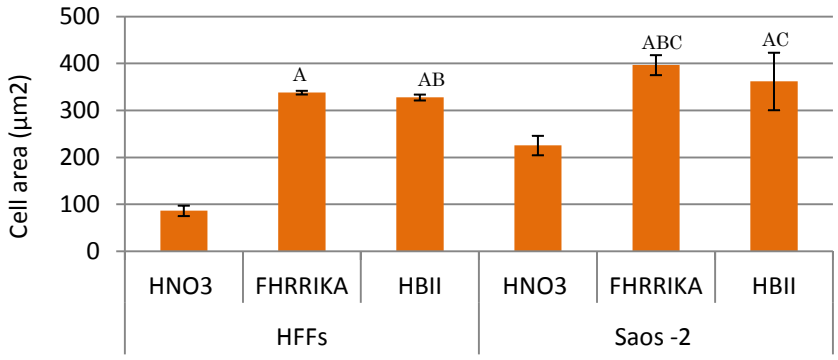

Figure 20 Adhesion test: cell spreading of Saos-2 and HFFs cells on Ti surfaces. Same letter indicates no statistically significant differences ($P < 0.05$) among the conditions.

These results are consistent with previous studies with osteoblasts cells; Rezania and Healy (1999) demonstrated that surfaces functionalized with FHRRIKA do not promote the spreading of rat calvaria osteoblast-like cells [14], and Dalton et al. (1995) demonstrated that osteoblasts-like bone derived cells cultured on the heparin-binding fragment showed only minimal spreading [16].

The results found in the current project support that interaction with the cell-binding domain is required for optimal spreading.

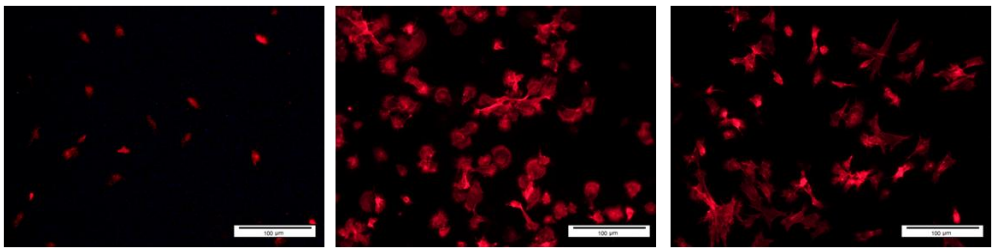

Figure 21 Cell spreading of HFFs cells on Ti surfaces; from left to right: Ti HNO3, Ti FHRRIKA, Ti HB II

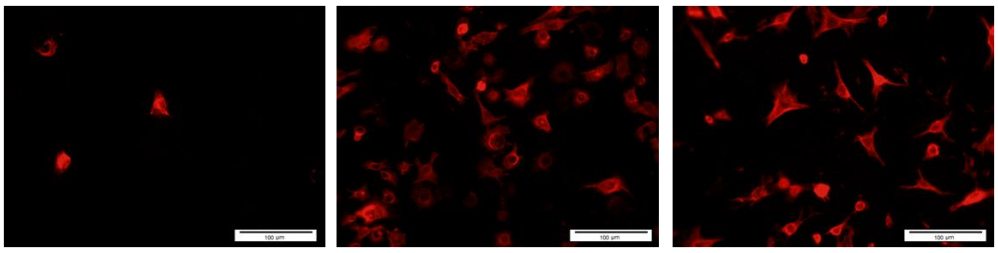

Figure 22 Cell spreading of Saos-2 cells on Ti surfaces; from left to right: Ti HNO3, Ti FHRRIKA, Ti HB II

Focal adhesions are central elements in the adhesion process, functioning as structural links between the cytoskeleton and extracellular matrix to mediate stable adhesion and migrations. [31]

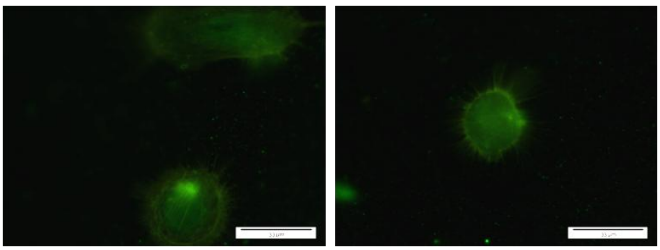

Figure 23 Focal adhesions of HFFs cells on Ti surfaces; Ti FHRRIKA (left) and Ti HB II (right)

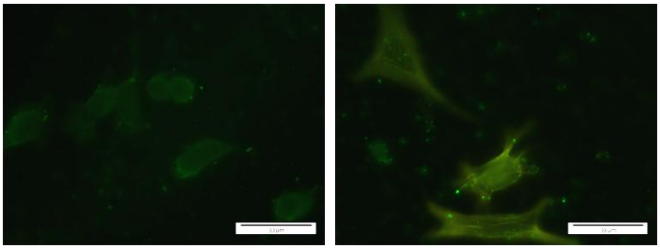

Figure 24 Focal adhesions of Saos-2 cells on Ti surfaces; Ti FHRRIKA (left) and Ti HB II (right)

Images of focal adhesion after 5h incubation are illustrated in Figure 23 and Figure 24. It was not possible to detect any focal adhesions in any cell type for controls surfaces or samples functionalized with the peptide. Only in the surfaces with protein fragment and with osteoblasts seeded was possible to see discrete focal adhesions. Rezania and Healy (1999) did not detect focal contact sides in the surfaces functionalized with FHRRIKA [14]; which is coherent with the results obtained in the current project.

12.2. Proliferation assay

Cell proliferation was followed for 14 days, quantifying cell numbers at day 1, 3, 7 and 14.

For HFFs cells all biofunctionalized surfaces have a high proliferation-capacity compared to uncoated controls (Figure 25). The highest values of cell proliferation were obtained for surfaces coated with the protein fragment after 14 days of incubation.

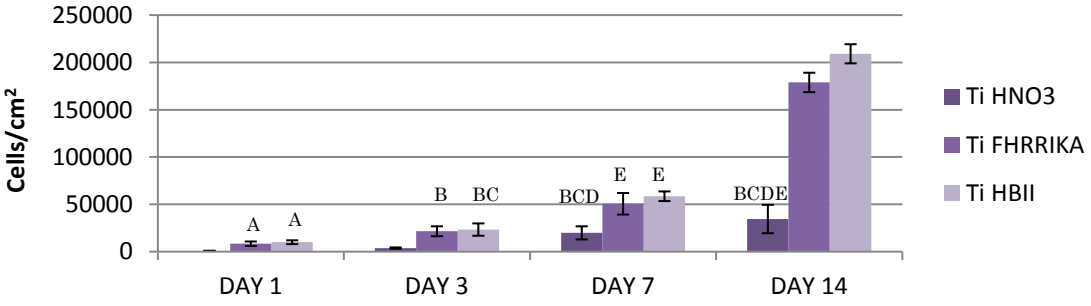

Figure 25 HFFs cells proliferation on Ti surfaces. Same letter indicates no statistically significant differences ($P < 0.05$) between groups.

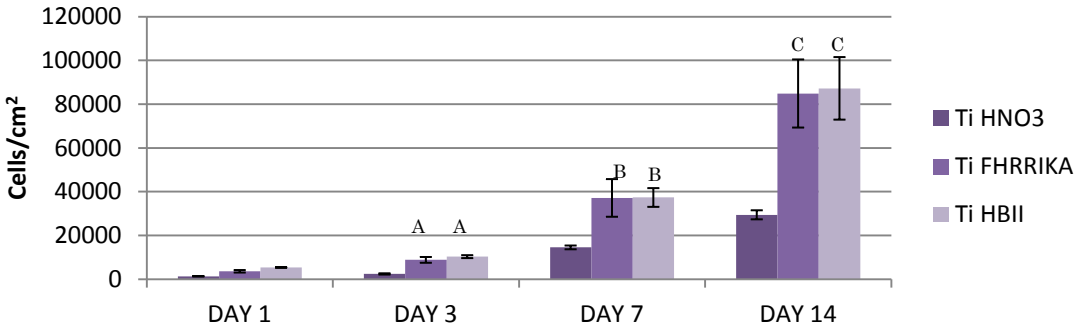

Figure 26 Saos-2 cells proliferation on Ti surfaces. Same letter indicates no statistically significant differences (P < 0.05) among the conditions.

For Saos-2 cells, both biofunctionalized surfaces supported a good proliferation-capacity compared to controls (Figure 26). For this cell system no statistically significant differences were observed between the peptide and the protein. In a previous study, Schuler et al. (2009) demonstrated the proliferation capacity on surfaces biofunctionalized with FHRRIKA, with higher amounts of osteoblasts (rat calvarial osteoblasts) than fibroblasts (human gingival fibroblasts) [32], which is different from our results.

Cellular behavior of Saos-2 on both biofunctionalized surfaces has similar results at short and long incubation periods. Thus, either the use of heparin-binding peptides or proteins represent successful strategies of biofunctionalization for enhancing the response of osteoblastic cells.

Alternatively, while HFFs showed an initial preference for surfaces biofunctionalized with the peptide, at long incubation times this tendency changes, reaching higher amounts of cells in the surfaces coated with the protein fragment than those coated with the peptide ones.

Short times are crucial for the colonization of the material, if osteoblasts have preference for protein fragment, they could proliferate faster and avoid the fibroblasts proliferation. This can be analyzed doing a co-culture assay, seeding both cell types simultaneously.

12.3. Gene expression assay

When fibroblasts are recruited at an injured site they are activated to a transient state named myofibroblasts. Myofibroblasts express alpha smooth muscle actin (ACTA2), a characteristic smooth muscle cell marker that confers cytoskeleton contractility, and synthesizes and remodels the ECM until they resolve the wound [30]. This marker is important at short time periods and is also important that the signal diminishes at long time periods to avoid fibrosis. In Figure 27 gene expression of ACTA2 is shown. All the titanium surfaces analyzed express a

similar amount of this gene, being higher at the beginning of the incubation for both biofunctionalized surfaces which is favorable for HFFs.

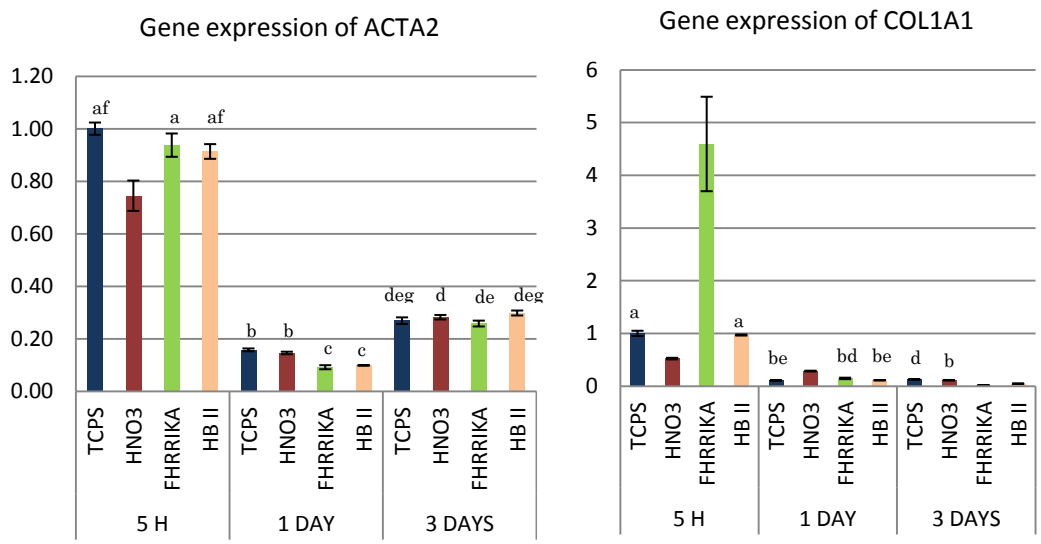

Figure 27 HFFs gene expression of ACTA2 (left) and COL1A1 (right) in titanium surfaces. Results were normalized in respect to expression levels of the endogen reference gene β-actin and are represented as relative fold change to tissue culture polystyrene (TCPS) at 5h. Same letter indicates no statistically significant differences ($P < 0.05$) among the conditions.

Following a tissue injury, fibroblasts play a critical role in the formation of collagen, which proliferate and produce a provisional matrix. However, it is also important that the signal diminishes at long time periods to avoid fibrosis, such as happens with ACTA2.

In Figure 27 is shown the expression of fibroblasts collagen type I (COL1A1). Surfaces biofunctionalized with the protein fragment do not express high amounts of this gene at 5h time, while functionalization with peptide shows really high values of collagen expression at this period time. This result can be associated with the good values of cell adhesion observed in the previous experiments (see Figure 19). After 3 days of incubation the expression of this gene is stopped on all surfaces, as expected, to avoid fibrosis.

After initial deposition of ECM components, myofibroblasts secrete matrix metalloproteinases (MMPs). MMPs play a central role in tissue remodelling and wound healing. In Figure 28 fibroblasts gene expression of MMP2 is shown. For this gene is important to study its expression at longer incubation times, because this gene is activated when ECM has been secreted. The surfaces biofunctionalized with the peptide display higher values of expression after 3 days of cell culture, which is correlated with a higher secretion of collagen (Figure 27).

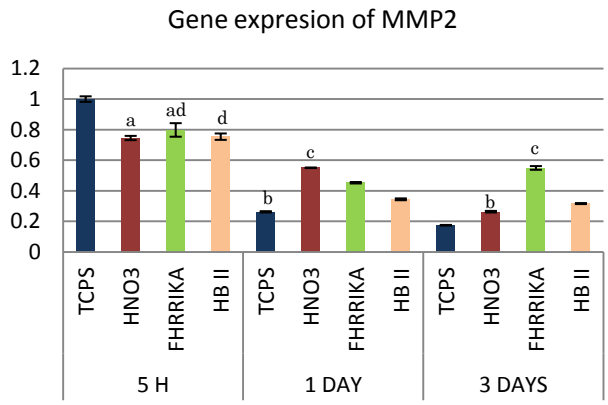

Figure 28 HFFs gene expression of MMP2 in titanium surfaces. Results were normalized in respect to expression levels of the endogen reference gene β-actin and are represented as relative fold change to tissue culture polystyrene (TCPS) at 5h. Same letter indicates no statistically significant differences ($P < 0.05$) among the conditions.

In summary, gene expression analysis on HFFs has shown better results in terms of gene activation for the surfaces functionalized with FHRRIKA peptide, this is directly correlated with a higher amount of fibroblasts attached compared to surfaces biofunctionalized with the protein fragment (Figure 19).

Osteoblasts secrete and mineralize the bone matrix. During adhesion and proliferation, several ECM proteins are secreted, such as collagen. In Figure 29 Saos-2 gene expression of COL1A1 is shown. The surfaces biofunctionalized with peptide have higher values than the other conditions studied in all the periods.

Moreover, the matrix maturation phase is characterized by the expression of alkaline phosphatase (ALP). ALP expression is shown in Figure 30. In this case, such as collagen, this gene is expressed at short times of incubation, and the higher value corresponds to samples functionalized with FHRRIKA.

BMP-2 like other bone morphogenetic proteins is involved in osteoblasts differentiation, and it is auto-secreted during osteogenic differentiation. The expression of this gene is important at long times of incubation. In Figure 29 can be observed that surfaces functionalized with peptide have the highest values of BMP-2 expression, also there is a significant increase in the surfaces functionalized with protein fragment.

Proteins such as osteocalcin (OSC) or bone sialoprotein are expressed once mineralization is completed, then it is important to study gene expression at long times of incubation (in our study 3 days). As illustrated in Figure 30 the biofunctionalized surfaces display higher expression of this gene at 3 days compared to controls, being clearly higher for the peptide-coated surfaces than for the protein-coated.

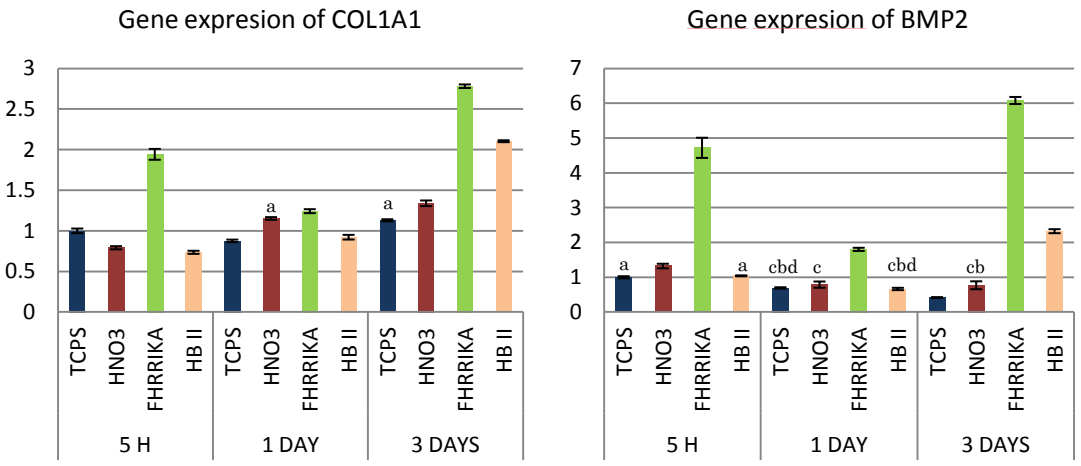

Figure 29 Saos-2 gene expression of COL1A1 (left) and BMP2 (right) in titanium surfaces. Results were normalized in respect to expression levels of the endogen reference gene ß-actin and are represented as relative fold change to tissue culture polystyrene (TCPS) at 5h. Same letter indicates no statistically significant differences (P < 0.05) among the conditions.

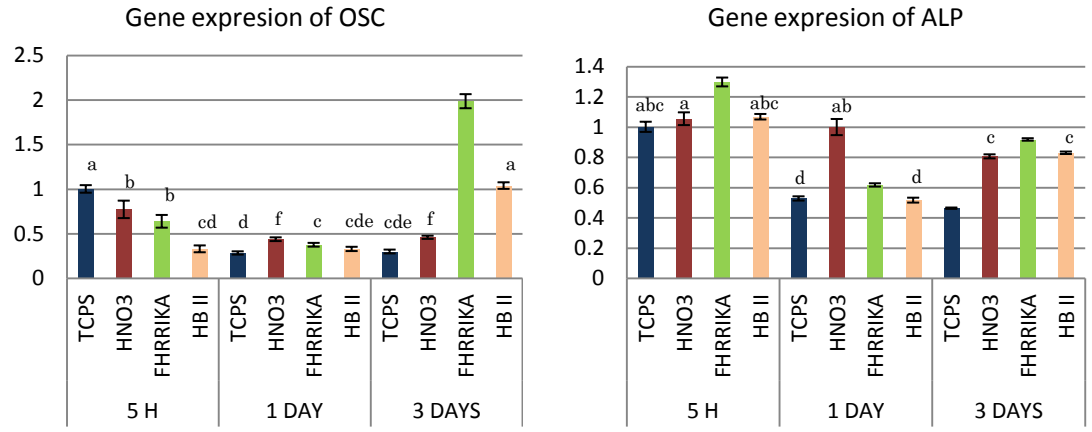

Figure 30 Saos-2 gene expression of OSC (left) and ALP (right) in titanium surfaces. Same letter indicates no statistically significant differences (P < 0.05) among the conditions.

The study of the expression of four genes related to osteoblastic activity and mineralization in Saos-2 cells has shown, in general, that surfaces functionalized with FHRRIKA stimulates the expression of these genes compared to control surfaces or surfaces coated with the protein. However, this peptide also enhanced the activity of HFFs cells, and thus is not selectively stimulating osteoblasts.

However, protein fragment stimulates osteoblastic differentiation genes (not as much as peptide) and at the same time does not stimulate fibroblastic activation genes.

This fact, and some selectivity in favour of binding Saos-2, makes this strategy interesting. Even more, if the process of functionalization could be optimized to get

the entire protein fragment bound covalently to titanium, which did not happen as mentioned in the stability analysis.

Chapter 4

Environmental impact analysis

The environmental impact of the project is due to the utilization of energy (oven, electricity...), water, biological material and chemical reactives. At each moment, it has been intended to minimise the quantity of resources, realise a correct management of the residues and adopt the general safety rules (appropriate clothing, personal protective equipment, not working alone...) in accordance with the material safety data sheets.

The experiments have been performed in the laboratory of Biomaterial of the Escola Tècnica Superior d'Enginyeria de Barcelona (ETSEIB), the Center for Research in NanoEngineering of UPC (CRnE) and in the Institute for Bioengineering of Catalonia (IBEC) located in the Parc Científic de Barcelona (PCB). In all places, the management of the residues and the storage of the reactives have been done in accordance with their internal rules.

In all the laboratories the residues are eliminated in different waste disposal following their nature:

- Sharp or pointed objects items contaminated that can cut or pierce (Needles, pointed objects, slides, glass Pasteur pipettes...)
- Cytotoxic and cytostatic biologic waste (Chemical substances and all materials that had been in contact with this kind of substances.)
- Biohazardous waste: All biological waste that could potentially cause harm to human/ animal health or environment (cell cultures, recombinant DNA...)
- No halogenated solvents (acetone, ethanol, 2-propanol, DMF, toluene and so on)
- Acid solutions, pH<7 (acid nitric)
- Solid waste (dirty paper, surface protection papers, aluminium foil...)

In the UPC laboratories, the full recipients are stocked in a security cupboard and each 6 months, the ECOCAT firm collects the laboratory wastes and realizes the process of waste management.

In the PCB the collect of the waste cans is weekly realized by their personnel.

Chapter 5

Conclusions

The successful biofunctionalization of titanium surfaces with FHRRIKA and HB II has been corroborated by physico-chemical characterization. The stability study of the biomolecules on the surfaces reveals that the binding of the peptide is stable, but also that some protein fragments are not covalently bound on the titanium surfaces.

Biofunctionalized surfaces with peptide display the same levels of cell adhesion for Saos-2 and HFFs. In contrast, the protein fragment clearly shows a preferential binding-capacity for Saos-2 cells. Surfaces biofunctionalized support but hardly promote the spreading of adherent cells.

At longer incubation periods, both biofunctionalized surfaces promoted the proliferation of Saos-2 and HFFs to a similar extent.

In the current study surfaces functionalized with the peptide stimulated in Saos-2 cell specific genes related to osteoblastic activity. However, the sequence FHRRIKA also stimulated HFFs activity. Thus, this peptide is not selective activating osteoblast functions.

On the other hand, protein fragment stimulates osteoblastic differentiation genes (not as much as peptide) and at the same time does not stimulate fibroblastic activation genes.

Bibliography

[1] Dillow A, Lowman A. Mimetic PeptideModified Materials for Control of Cell Differentiation. Biomim. Mater. Des. Biointerfacial Strateg. Tissue Eng. Target. Drug Deliv., CRC Press; 2002.

[2] S.Anil, P.S. Anand HA and JAJ. Dental Implant Surface Enhancement and Osseointegration. Implant Dent., 2011, p. 83–108.
Available from: http://www.intechopen.com/books/implant-dentistry-a-rapidly-evolving-practice/dental-implant-surface-enhancement-and-osseointegration

[3] Mavrogenis AF, Dimitriou R, Parvizi J, Babis GC. Biology of implant osseointegration 2009;9:61–71.

[4] Özcan M, Hämmerle C. Titanium as a Reconstruction and Implant Material in Dentistry: Advantages and Pitfalls. Materials (Basel) 2012;5:1528–45.

[5] Kulkarni M, Mazare A, Schmuki P, Iglič A. Biomaterial surface modification of titanium and titanium alloys for medical applications. Nanomedicine, 2014, p. 111–36.

[6] Schuler M, Trentin D, Textor M, Tosatti S. Biomedical interfaces: titanium surface technology for implants and cell carriers. Nanomedicine 2006;1:449–63.

[7] Takao Hanawa. A comprehensive review of techniques for biofunctionalization of titanium. J Periodontal Implant Sci 2011;41:263–72.

[8] Schliephake H, Scharnweber D. Chemical and biological functionalization of titanium for dental implants. J Mater Chem 2008;18:2404.

[9] Shekaran A, García AJ. Extracellular matrix-mimetic adhesive biomaterials for bone repair. J Biomed Mater Res 2011;96A:261–72.

[10] Kim H-E, Kim H-W, Jang J-H. Identification and characterization of a novel heparin-binding peptide for promoting osteoblast adhesion and proliferation by screening an Escherichia coli cell surface display peptide library. J Pept Sci 2009;15:43–7.

[11] Shin H, Jo S, Mikos AG. Biomimetic materials for tissue engineering. Biomaterials 2003;24:4353–64.

[12] Kay C. Dee, Thomas T. Andersen, Rena Bizios. Design and function of novel osteoblast-adhesive peptides for chemical modification of biomaterials. J Biomed Mater Res 1998;40:371–7.

[13] Tsai W-B, Chen RP-Y, Wei K-L, Chen Y-R, Liao T-Y, Liu H-L, et al. Polyelectrolyte multilayer films functionalized with peptides for promoting osteoblast functions. Acta Biomater 2009;5:3467–77.

[14] Rezania A, Healy KE. Biomimetic Peptide Surfaces That Regulate Adhesion, Spreading, Cytoskeletal Organization, and Mineralization of the Matrix Deposited by Osteoblast-like Cells. Biotechnol Prog 1999;15:19–32.

[15] Gui L, Wojciechowski K, Gildner CD, Nedelkovska H, Hocking DC. Identification of the Heparin-binding Determinants within Fibronectin Repeat III1: ROLE IN CELL SPREADING AND GROWTH. J Biol Chem 2006;281:34816–25.

[16] Dalton BA, Mcfarland CD, Underwood PA, Steele JG. Role of the heparin binding domain of fibronectin in attachment and spreading of human bone-derived cells 1995;2092:2083–92.

[17] Broggini N, Tosatti S, Ferguson SJ, Schuler M, Textor M, Bornstein MM, et al. Evaluation of chemically modified SLA implants (modSLA) biofunctionalized with integrin (RGD)- and heparin (KRSR)-binding peptides. J Biomed Mater Res A 2012;100:703–11.

[18] J. Cl. Puippe. Surface treatments of titanium implants. Eur Cells Mater 2003;5:32–3.

[19] Mas-Moruno C, Fraioli R, Albericio F, Manero JM, Gil FJ. Novel Peptide-Based Platform for the Dual Presentation of Biologically Active Peptide Motifs on Biomaterials. ACS Appl Mater Interfaces 2014;6:6525–36.

[20] Díez CH. Functionalization of a Ti-based Alloy with Synthesized Recombinant Fibronectin Fragments to Improve Cellular Response 2014.

[21] Menzies KL, Jones L. The Impact of Contact Angle on the Biocompatibility of Biomaterials. Optom Vis Sci 2010;87:1.

[22] Kwok D., Neumann A. Contact angle interpretation in terms of solid surface tension. Colloids Surfaces A Physicochem Eng Asp 2000;161:31–48.

[23] Robert J. Good, Carel J. van Oss. The Modern Theory of Contact Angles and the Hydrogen Bond Components of Surface Energies. Mod. Approaches to Wettability, Springer US; 1992, p. 1–27.

[24] Chong WK, Li X, Soh YC. Phosphor-Based White Light Emitting Diode (LED) for Vertical Scanning Interferometry (VSI) n.d.

[25] Gadelmawla ES, Koura MM, Maksoud TMA, Elewa IM, Soliman HH. Roughness parameters. J Mater Process Technol 2002;123:133–45.

[26] Zhou W, Apkarian R, Wang Z, Joy D. Fundamentals of Scanning Electron Microscopy (SEM). Scanning Microsc. Nanotechnol., Springer New York; 2007, p. 1–40.

[27] Jagtap RN, Ambre AH. Overview literature on atomic force microscopy (AFM): Basics and its important applications for polymer characterization 2006;13:368–84.

[28] Hofmann S. Introduction and Outline. Auger- X-Ray Photoelectron Spectrosc. Mater. Sci., Springer Berlin Heidelberg; 2013, p. 1–10.

[29] Hausser H-J, Brenner RE. Phenotypic instability of Saos-2 cells in long-term culture. Biochem Biophys Res Commun 2005;333:216–22.

[30] Guillem-Marti J, Delgado L, Godoy-Gallardo M, Pegueroles M, Herrero M, Gil FJ. Fibroblast adhesion and activation onto micro-machined titanium surfaces. Clin Oral Implants Res 2013;24:770–80.

[31] Garcia a. J, Reyes CD. Bio-adhesive Surfaces to Promote Osteoblast Differentiation and Bone Formation. J Dent Res 2005;84:407–13.

[32] Schuler M, Hamilton DW, Kunzler TP, Sprecher CM, de Wild M, Brunette DM, et al. Comparison of the response of cultured osteoblasts and osteoblasts outgrown from rat calvarial bone chips to nonfouling KRSR and FHRRIKA-peptide modified rough titanium surfaces. J Biomed Mater Res Part B Appl Biomater 2009;91B:517–27.

Budget

The present section presents the global cost of this project. The economic study includes the equipment used, human resources and the material costs. The fees are calculated based on a Junior Engineer.

Table 6 Raw material

	Amount	Price	Cost
Titanium discs grade 2 diameter 10mm, 2mm thick	150	0,09901€/mm	**29,70€**

Table 7 Samples preparation

	Amount	Price	Cost
SiC Paper P800	16u	1,27€/u	20,32€
SiC P1200	16u	1,67€/u	26,72€
Velvet polishing cloth	2u	5,80€/u.	11,60€
Alumina 0.05 micron buehler	0,2kg	134,70€/kg	26,94€
Alumina 1 micron buehler	0,2kg	134,70€/kg	26,94€
Buehler Phoenix 4000 sample preparation system	24h	30,00€/h	720,00€
TOTAL			**832,52 €**

Table 8 Samples cleaning

	Amount	Price	Cost
Cyclohexane	0,31l	50,30€/l	15,59€
2-propanol	0,49l	19,76€/l	9,68€

Acetone	0,79l	15,48€/l	12,23€
Ethanol	0,79l	12,99€/l	10,26€
Distilled water	7,09l	0,08€/l	0,57€
TOTAL			**48,33€**

Table 9 Surface passivation

	Amount	**Price**	**Cost**
HNO_3	0,12l	16,33€/l	1,96€
TOTAL			**1,96€**

Table 10 Physico-chemical characterization

	Amount	**Price**	**Cost**
VSI	2h	80,00€/h	160,00€
Contact angle	6h	14,40€/h	86,40€
AFM	6h	130,00€/h	780,00€
SEM	1h	130,00€/h	130,00€
XPS	18 samples	240€/sample	4.320,00€
TOTAL			**5.476,40€**

Table 11 Functionalization

	Amount	**Price**	**Cost**
APTES	0,0018l	580,00€/l	1,04€
Cross linker	0,090g	349,60€/g	31,46€
Toluene	0,31l	61,00€/l	18,91€
DMF	0,31l	136,60€/l	42,35€
Peptide FHRRIKA	1u	200,00€/u	200,00€
Protein fragment HB II	1u	200,00€/u	200,00€
TOTAL			**493,76€**

Table 12 Biological characterization

	Amount	Price	Cost
PBS	4u.	1,56€/u.	6,24€
McCoy medium	0,520l	44,80€/l	23,30€
DMEM medium	0,526l	62,00€/l	32,61€
HEPES (1M)	0,024l	1104,50€/l	26,51€
FBS	0,100l	88,40€/l	8,84€
Sodium pyruvate	0,006l	84,20€/l	0,51€
Penicillin/streptomycin	0,012l	125,00€/l	1,50€
L-glutamine	0,012l	105,20€/l	1,26€
Trypsin	0,040l	69,28€/l	2,77€
BSA	3,0g	2,17€/g	6,51€
PFA	0,006l	9744,00€/l	58,46€
M-PER	0,036l	783,88€/l	28,22€
Culture hood	50h	10,00€/h	500,00€
Glycine	0,225g	1,02€/g	0,23€
Triton	0,025ml	381,00€/l	0,01€
Mouse Anti-vinculin	0,018ml	132,50€/ml	2,39€
Goat Alexa 488	0,009ml	1472,00€/ml	13,25€
Alexa Fluor 546 Phalloidin	0,006ml	426,00€/ml	2,56€
DAPI	0,009ml	1650,00€/mL	14,85€
Mowiol	5,00g	0,50€/g	2,50€
Fluorescence microscope	6h	60,00€/h	360,00€
Cytotoxicity Detection Kit	1/10Kit	600,70€/Kit	60,07€
AlamarBlue Cell Viability Reagent	0,010l	8.440,00€/l	84,40€
Microplate Fluorescence Reader	0,5h	7,64€/h	3,82€
Spectrophotometer PowerWave XS Microplate	0,5h	7,64€/h	3,82€
RNeasy Mini Kit (50)	1/10Kit	307,00€/kit	30,70€

QuantiTect Reverse Transcription Kit (50)	1/10Kit	307,00€/kit	30,70€
PCR human primers	9 · 1/20primer	12€/primer	5,40€
TOTAL			**1.307,61€**

Table 13 Other costs

	Amount	**Price**	**Cost**
Office material, printings, CD, files…			200,00€
Consumable lab material			150,00€
Common lab equipment, milliQ water, paper, …			100,00€
Junior Engineer	720h	20,00€/h	14.400,00€
TOTAL			**14.850,00€**

Table 14 Final costs

Concept	**Total Cost**
Cost associated with raw material	29,70€
Cost associated with sample preparation	832,52 €
Cost associated with sample cleaning	48,33€
Cost associated with surface passivation	1,96€
Cost associated with physico-chemical characterization	5.476,40€
Cost associated with functionalization	493,76€
Cost associated with biological characterization	1.307,61€
Cost associated with other costs	14.850,00€
Subtotal	**23.040,28€**
V.A.T. (21%)	**4.838,46€**
TOTAL AMOUNT	**27.878,74€**